Electronic Supporting information

High-performance SERS substrate based on perovskite quantum dot-graphene/nano-Au composites for ultrasensitive detection of rhodamine 6G and p-nitrophenol

Jiangcai Wang,[a] Cuicui Qiu,*[a] Hua Pang,[a] Junyu Wu,[b] Mengtao Sun*[c] and Dameng Liu*[ad]

[a] *State Key Laboratory of Tribology, Tsinghua University, Beijing 100084, China*

[b] *Electronic Information Science and Technology, School of Physics and Electronics, Central South University, Hunan 410083, China*

[c] *School of Mathematics and Physics, University of Science and Technology Beijing, Beijing 100083, China*

[d] *Tianjin Research Institute for Advanced Equipment, Tsinghua University, Tianjin 300300, China*

** Corresponding Authors*
Cuicui Qiu, email: cuicuiqiu@aliyun.com
Mengtao Sun, email: mengtaosun@ustb.edu.cn
Dameng Liu, Tel: 86-10-62797646; email: ldm@tsinghua.edu.cn

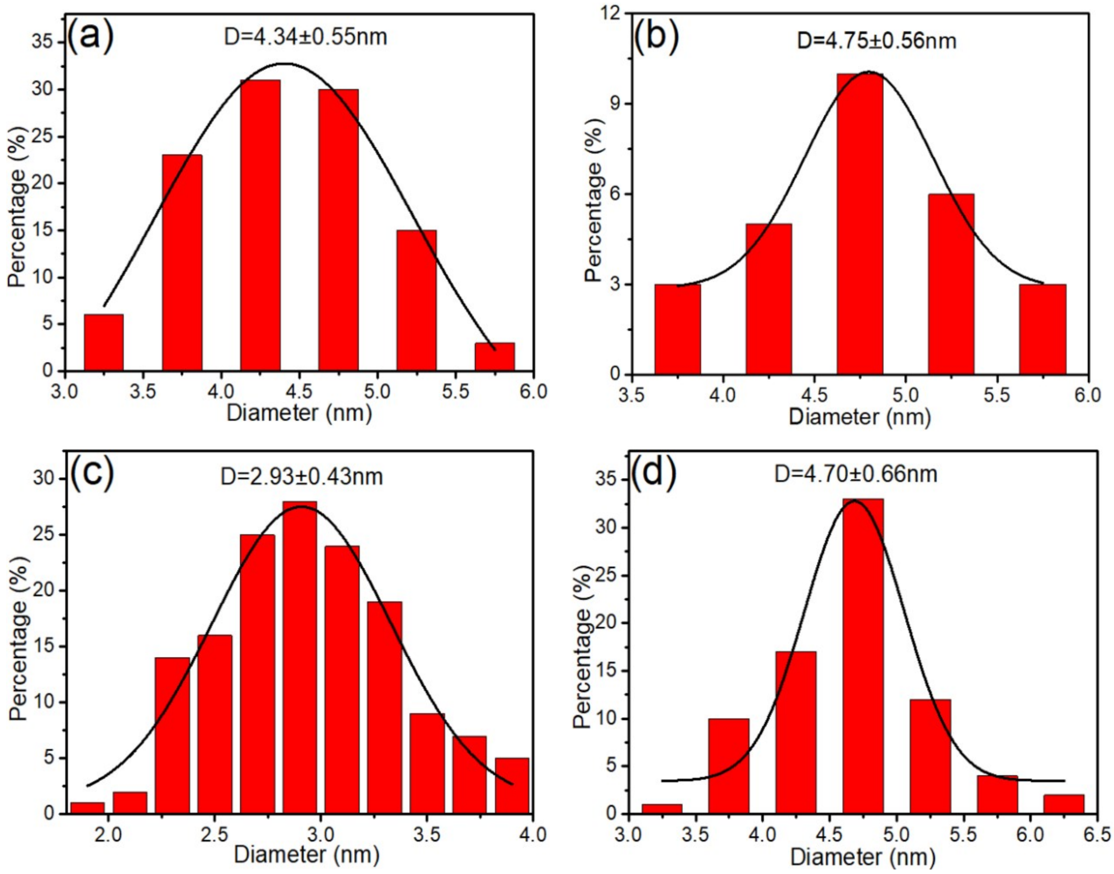

Fig. S1 The average diameter of PQDs distributed on the Graphene with the synthesis conditions of $MABr/PbBr_2$=4/5 (a), $MABr/PbBr_2$=6/5 (b) with a fixed value of oleylamine/oleic acid (1/25), and oleylamine/oleic acid =1/1 (c), oleylamine/oleic acid =1/50 (d) with a fixed value of $MABr/PbBr_2$ (5/5).

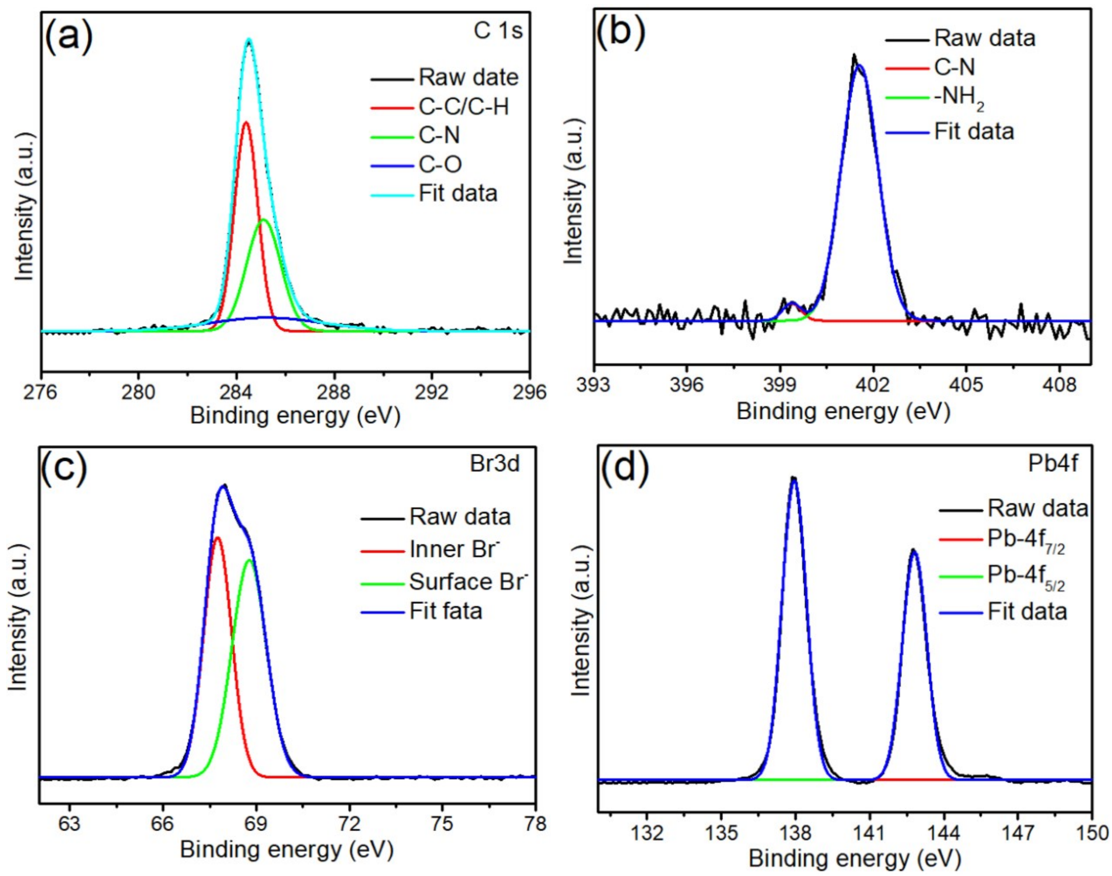

Fig. S2 XPS of pristine PQDs: C1s (a), N1s (b), Br3d (c), and Pb4f (d).

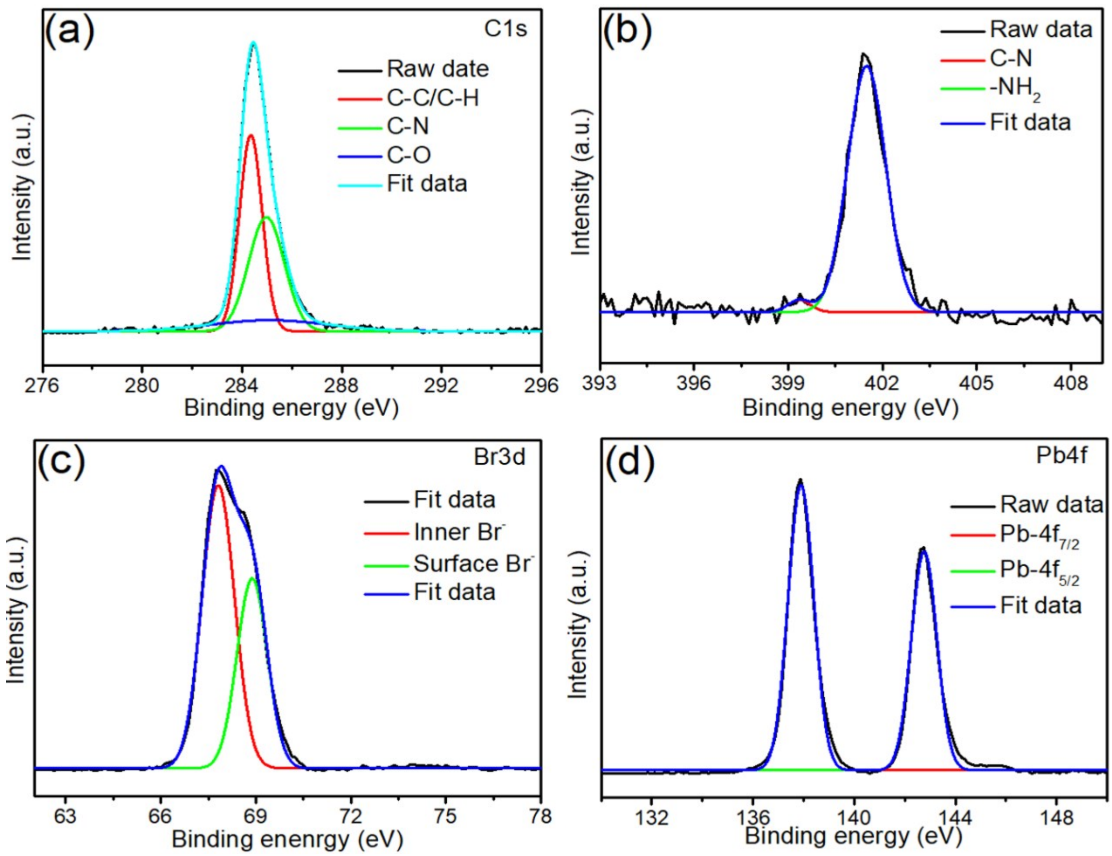

Fig. S3 XPS of hybrid PQD-G: C1s (a), N1s (b), Br3d (c), and Pb4f (d).

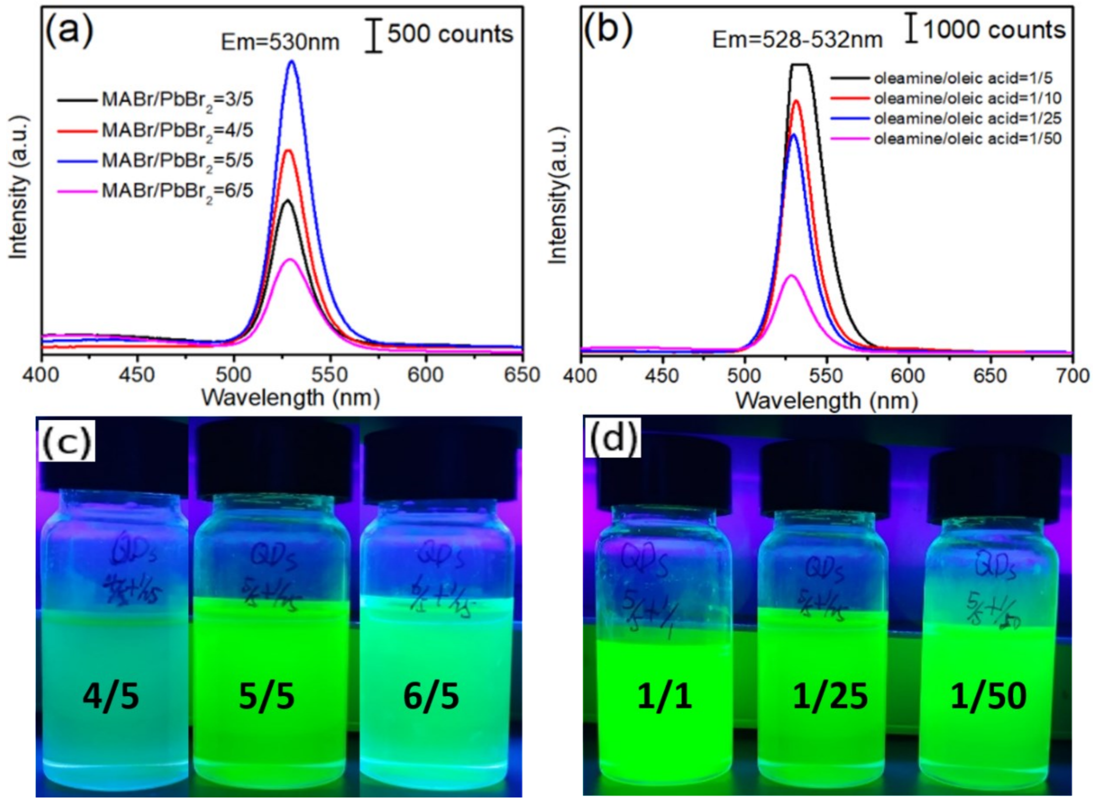

Fig. S4 (a) The emission spectrum of PQD under different molar ratios of $MABr/PbBr_2$ (from 3/5 to 6/5) with a fixed molar ratio of oleylamine/oleic acid (1/25). (b) The emission spectrum of PQD under different molar ratios of oleylamine/oleic acid (from 1/5 to 1/50) with a fixed molar ratio of $MABr/PbBr_2$ (5/5). The luminescence comparison of PQDs at the different molar ratios of (c) $MABr/PbBr_2$ with a fixed molar ratio of oleylamine/oleic acid (1/25) and (d) oleylamine/oleic acid with a fixed molar ratio of $MABr/PbBr_2$ (5/5), as taken by using a commercial phone camera under portable ultraviolet lamp illumination with 365 nm.

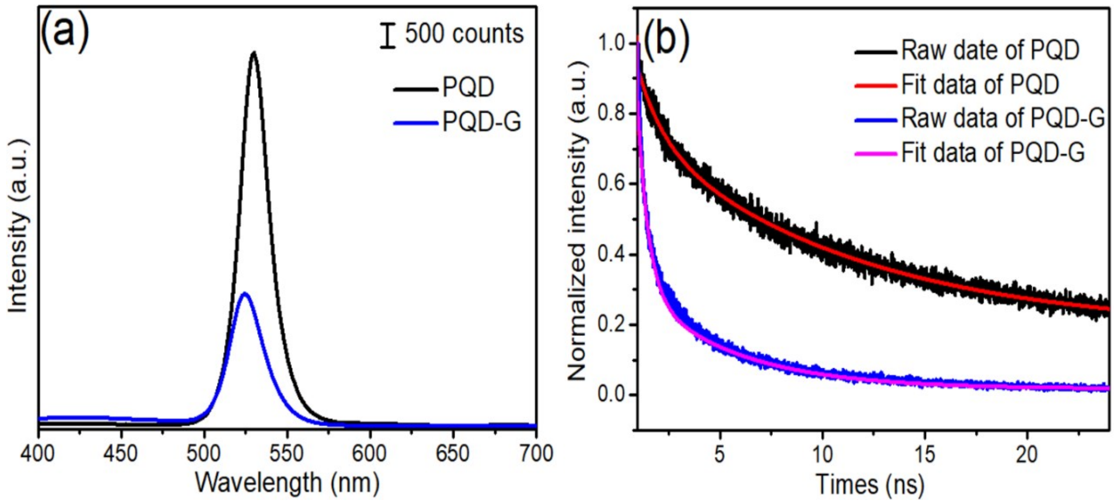

Fig. S5 (a) PL spectra of the PQD (black) and PQD-G (blue) at 365 nm. (b) PL decay profiles of PQD (black) and PQD-G (blue) at 488 nm.

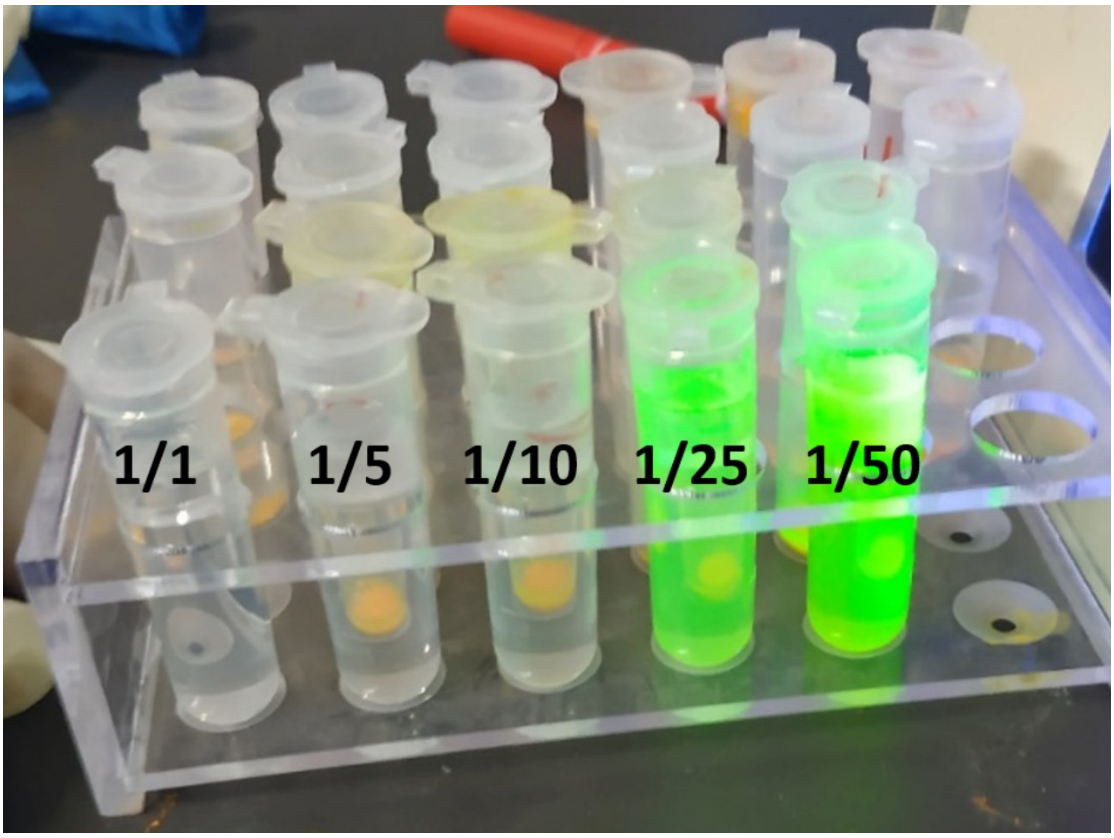

Fig. S6 The comparison of luminescent stability of PQDs at the different molar ratios of oleylamine/oleic acid with a fixed value of $MABr/PbBr_2$ (5/5) , which were kept at room temperature for about seven days, as taken by using a commercial phone camera under portable ultraviolet lamp illumination with 365 nm.

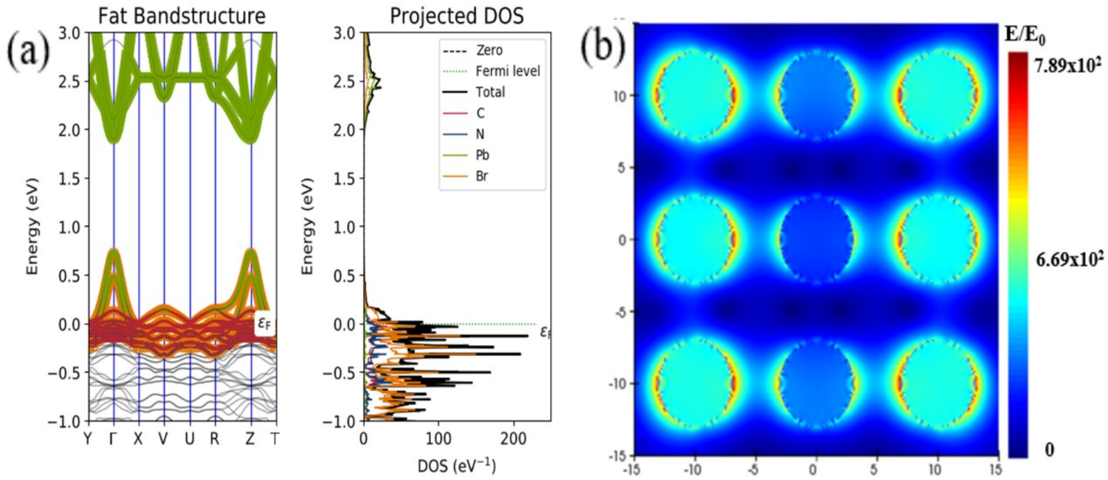

Fig. S7 (a) The electronic structure (energy) band and density of states of PQDs. (b) A simulated EM field distribution in a periodic SiO_2-Cr-Au-G-PQD layered array nanostructure with a fixed radius of PQD nanoparticles (2 nm), gap distance between nanoparticles (4 nm) and graphene thickness (1 nm) at 550 nm.

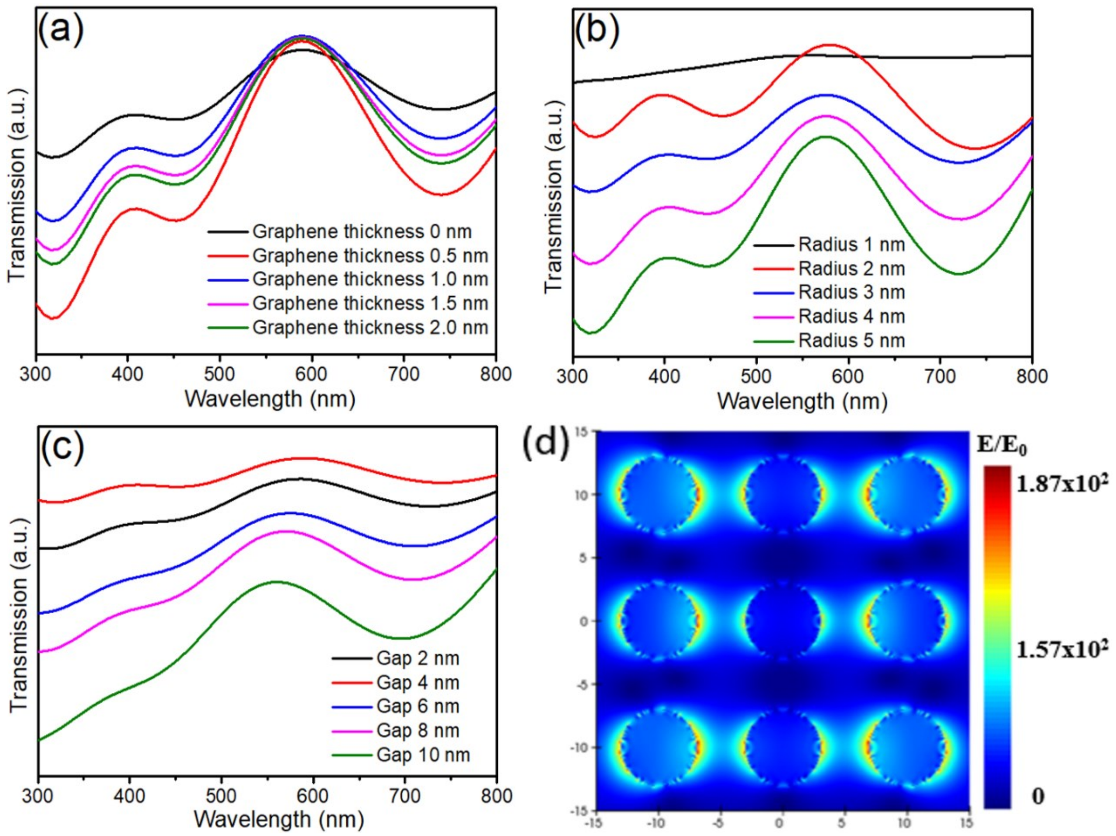

Fig. S8 A simulated transmission spectra with different synthesis parameters at different excitation wavelength. (a) The thickness of graphene-dependent transmission spectra in a periodic SiO_2-Cr-Au-G-PQD layered array nanostructure. (b) The radius of PQD-dependent transmission spectra in a periodic SiO_2-Cr-Au-G-PQD layered array nanostructure. (c) The gap distance between PQD nanoparticles-dependent transmission spectra in a periodic SiO_2-Cr-Au-G-PQD layered array nanostructure. (d) A simulated EM field distribution in a periodic SiO_2-Cr-Au layered array nanostructure at 633 nm.

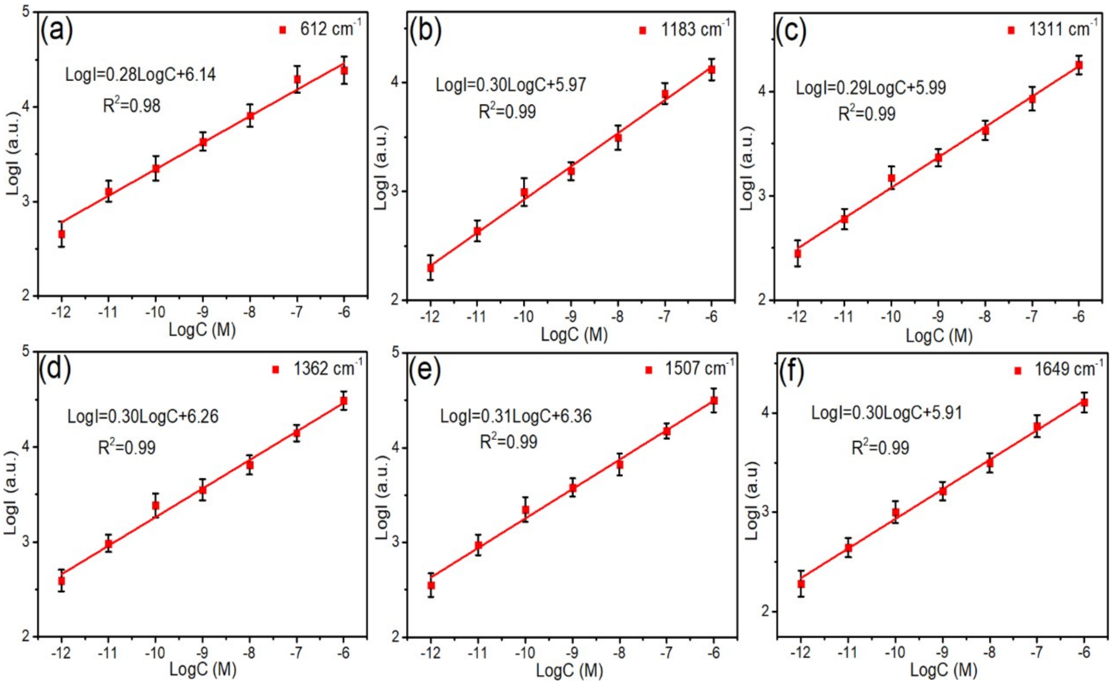

Fig. S9 Corresponding calibration plots of Fig. 5a for quantitative analysis of R6G at (a) 612 cm^{-1}, (b) 1183 cm^{-1}, (c) 1311 cm^{-1}, (d) 1362 cm^{-1}, (e) 1507 cm^{-1}, (f) 1649 cm^{-1}.

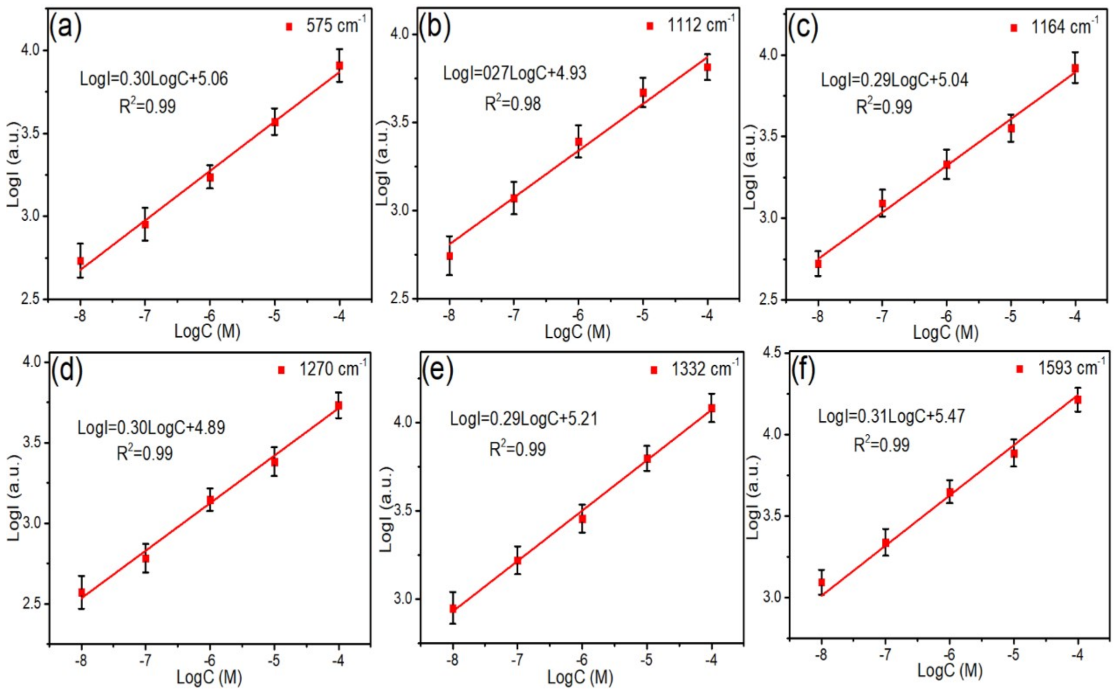

Fig. S10 Corresponding calibration plots of Fig. 5c for quantitative analysis of PNP at (a) 575 cm^{-1}, (b) 1112 cm^{-1}, (c) 1164 cm^{-1}, (d) 1270 cm^{-1}, (e) 1332 cm^{-1}, (f) 1593 cm^{-1}.

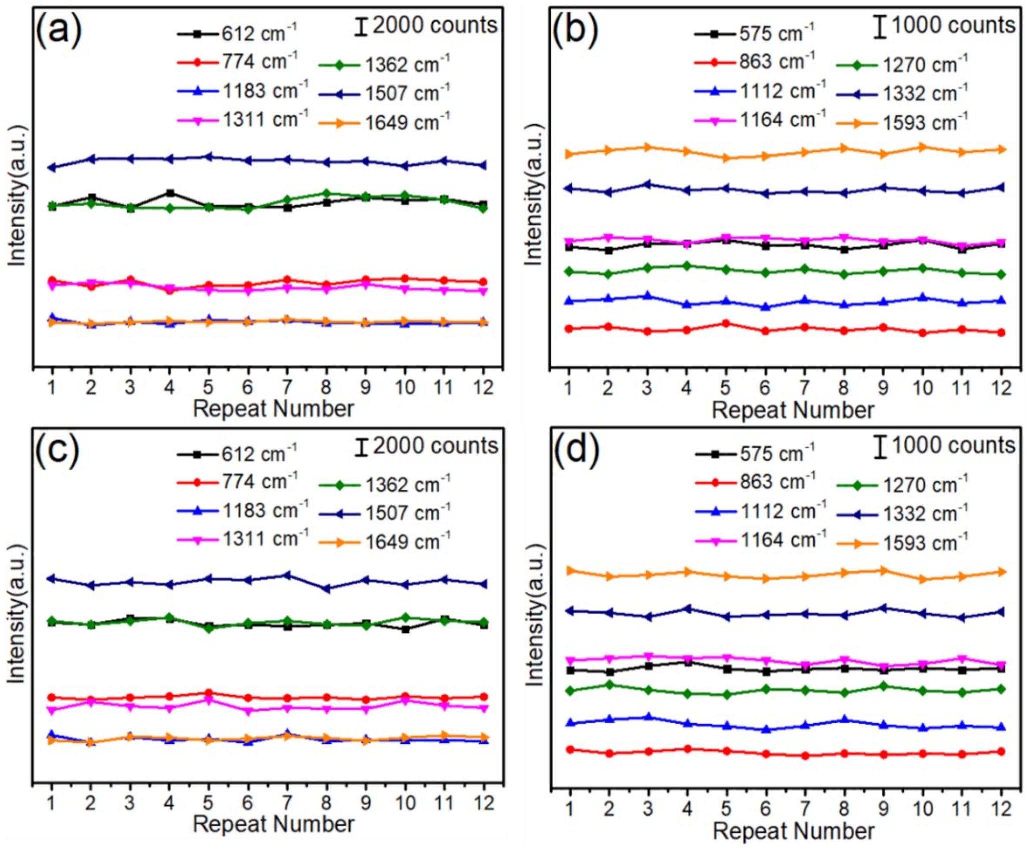

Fig. S11 SERS intensity responses of the PQD-G/Au for the characteristic peak of 10^{-6} M R6G on 12 random sites from the six different substrates (a) and from the same substrates (c). SERS intensity responses of the PQD-G/Au for the characteristic peak of 10^{-4} M PNP on 12 random sites from the different substrates (b) and from the same substrates (d).

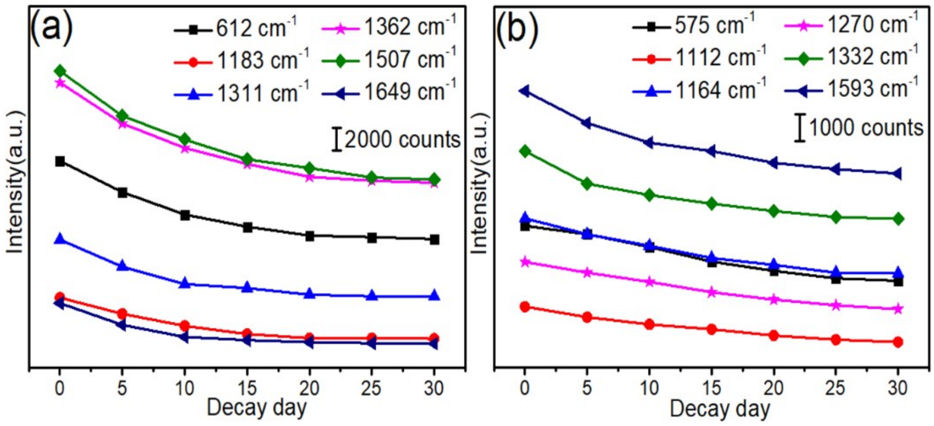

Fig. S12 The intensity change of other Raman peaks on the optimized PQD-G/Au composite over 30 days of 10^{-6} M R6G (a) and 10^{-4} M PNP (b).

Table S1 Comparison of detection limits and linear ranges for other SERS substrates.

SERS substrate	Preparation method	Target molecule	Detection range (M)	Detection limit (M)	EF	Ref
G@CuNP/G@Cu	CVD	R6G	10^{-9}~10^{-5}	10^{-9}	__	1
Au NP–G–Ag NA	EBL [a], EBD [b]	R6G	__	10^{-13}	6.9×10^{7}	2
GO/Ag/Psi [c]	Dip-coating, Hummers	R6G	10^{-4}~10^{-7}	10^{-7}	—	3
G/Ag/LTSi [d]	Laser Ablation, EBD	R6G	10^{-6}~10^{-11}	10^{-10}	2.6×10^{7}	4
GO/Au	CVD	R6G	—	10^{-7}	1.2×10^{7}	5
AuNPs/rGO	Hydrothermal	Pb^{2+}	10^{-9}~10^{-6}	10^{-9}	—	6
G@AgNPs@Si	Hydrothermal, Electrochemical technology	R6G, Bacteria	—	10^{-9}	8.3×10^{6}	7
GO/AuNR	A seed-mediated method, modified Hummers method	Rhodamine 640	—	10^{-9}	1.0×10^{4}	8
G/CuNPs	A two temperature zone CVD method	Adenosine	10^{-9}~10^{-7}	10^{-9}	—	9
haze/GO/Au	Two-step anodization techniques followed by wet-etching and drop-casting	R6G	10^{-3}~10^{-5}	_	3.3×10^{3}	10

[a] EBL is the abbreviation of Electron beam lithography.

[b] EBD is the abbreviation of Electron beam deposition.

[c] PSi is the abbreviation of /silicon pyramid arrays structure.

[d] LTSi is the abbreviation of Laser-Textured Si.

Table S2 Enhancement factor of characteristic peaks of R6G on the optimized PQD-G/Au substrates.

Peak (cm^{-1})	EF
612	3.15×10^{12}
1185	1.71×10^{12}
1311	4.68×10^{12}
1362	3.31×10^{12}
1507	3.57×10^{12}
1649	3.85×10^{12}

Supporting references

1. C. Yang, C. Zhang, Y. Huo, S. Jiang, H. Qiu, Y. Xu, X. Li and B. Man, *Carbon*, 2016.
2. Y. Zhao, X. Li, L. Zhang, B. Chu, Q. Liu and Y. Lu, *RSC Advances*, 2017, **7**, 49303-49308.
3. C. Zhang, S. Z. Jiang, Y. Y. Huo, A. H. Liu, S. C. Xu, X. Y. Liu, Z. C. Sun, Y. Y. Xu, Z. Li and B. Y. Man, *Opt. Express*, 2015, **23**, 24811-24821.
4. Z. Chentao, L. Kun, H. Yuanqing and Z. Jianhuan, *Sensors*, 2017, **17**, 1462.
5. X. Liang, B. Liang, Z. Pan, X. Lang, Y. Zhang, G. Wang, P. Yin and L. Guo, *Nanoscale*, 2015, **7**, 20188-20196.
6. Longyun, Zhao, Wei, Gu, Cuiling, Zhang, Xinhao, Shi, Yuezhong and Xian, *Journal of Colloid and Interface ence*, 2016, **465**, 279-285.
7. X. Meng, H. Wang, N. Chen, P. Ding, H. Shi, X. Zhai, Y. Su and Y. He, *Anal. Chem.*, 2018, acs.analchem.7b05139.
8. P. G. Vianna, D. Grasseschi, G. K. B. Costa, I. C. S. Carvalho, S. H. Domingues, J. Fontana and C. J. S. De Matos, *ACS Photonics*, 2016, acsphotonics.6b00109.
9. Shicai, Xu, Baoyuan, Man, Shouzhen, Jiang, Jihua, Wang, Jie and Wei, *Acs Applied Materials & Interfaces*, 2015.
10. S. Behera, J. Im and K. Kim, *ACS Applied Nano Materials*, 2019.